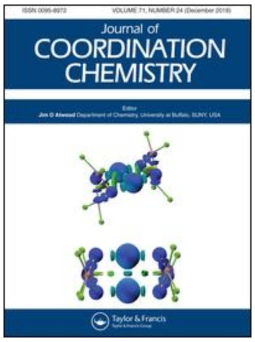

Journal of Coordination Chemistry

ISSN: 0095-8972 (Print) 1029-0389 (Online) Journal homepage: https://www.tandfonline.com/loi/gcoo20

Pd@GO/Fe_3O_4/PAA/DCA: a novel magnetic heterogeneous catalyst for promoting the Sonogashira cross-coupling reaction

Mansoureh Daraie, Majid M. Heravi & Shaghayegh Sadat Kazemi

To cite this article: Mansoureh Daraie, Majid M. Heravi & Shaghayegh Sadat Kazemi (2019): Pd@GO/Fe_3O_4/PAA/DCA: a novel magnetic heterogeneous catalyst for promoting the Sonogashira cross-coupling reaction, Journal of Coordination Chemistry, DOI: 10.1080/00958972.2019.1640360

To link to this article: https://doi.org/10.1080/00958972.2019.1640360

JOURNAL OF COORDINATION CHEMISTRY
https://doi.org/10.1080/00958972.2019.1640360

Pd@GO/Fe_3O_4/PAA/DCA: a novel magnetic heterogeneous catalyst for promoting the Sonogashira cross-coupling reaction

Mansoureh Daraie, Majid M. Heravi and Shaghayegh Sadat Kazemi

Department of Chemistry, School of Science, Alzahra University, Vanak, Tehran, Iran

ABSTRACT

A hybrid system involving graphene oxide (GO), magnetic oxide (Fe_3O_4), acrylamide and dicyandiamide was prepared via amine functionalization of GO/Fe_3O_4 by means of covalent bonding with acrylamide and subsequent reaction with dicyandiamide to provide a multinitrogen containing polymer on the surface of GO. This hybrid system was utilized as a heterogeneous catalyst support for immobilizing Pd nanoparticles to provide the hybrid, Pd@GO/Fe_3O_4/PAA/DCA. This nano-Pd composite was characterized using Fourier transform infrared, transmission electron microscopy, scanning electron microscopy, vibrating sample magnetometer, thermogravimetric analysis, X-ray diffraction, and ICP techniques and used for promoting Sonogashira cross-coupling under mild reaction conditions. This heterogeneous and magnetic catalyst was easily separated by external magnet and was reused in a model reaction, efficiently up to six times with slight loss of catalytic activity and Pd leaching, showing the suitability of GO/Fe_3O_4/PAA/DCA for embedding Pd nanoparticles. To check the effect of the number of surface nitrogens of the polymeric chain on the catalytic performance, the activity of the catalyst was compared with Pd@GO/Fe_3O_4/PAA; increased number of the surface nitrogens on the chain polymer leads to higher loading of Pd and lower the Pd leaching.

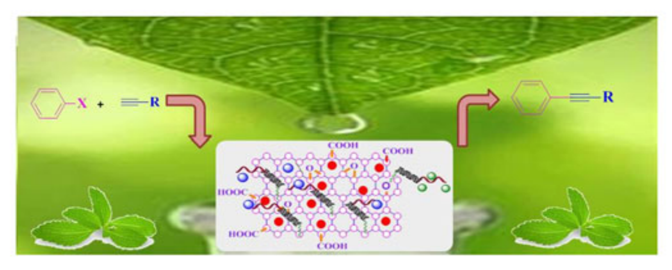

ARTICLE HISTORY
Received 20 April 2019
Accepted 21 June 2019

KEYWORDS
GO; Fe_3O_4; acrylamide; dicyandiamide; Pd nanoparticles; copper and ligand-free; Sonogashira cross-coupling reaction

CONTACT Majid M. Heravi ✉ mmh1331@yahoo.com

1. Introduction

Organic chemistry is responsible for numerous fascinating natural phenomena. By studying organic chemistry man has learnt how to augment nature's chemistry, how to build carbon-based functional molecules: drugs, plastics, and other high-technical materials [1]. Therefore, the art of carbon–carbon bond formation and especially cross-coupling C–C bond formation are important for synthetic organic chemists [2].

Pd-catalyzed cross-coupling reactions are numerous and the design of new homogeneous and heterogeneous palladium-based catalysts has attracted much attention [3–5]. Importance of this field has been proven by the Nobel Prize in Chemistry in 2010 to Richard F. Heck, Ei-ichi Negishi, and Akira Suzuki for their outstanding work on applications of palladium-catalyzed cross-coupling reactions [6]. Sonogashira reaction is another important Pd-catalyzed cross-coupling reaction; the alkynylation reaction of aryl halides using aromatic acetylenes was reported in 1975 in three independent contributions by Cassar [7], Dieck and Heck [8], as well as Sonogashira [9].

Sonogashira reaction is one of the most important and powerful methods for C–C bond formation involving the cross coupling between terminal sp hybridized carbon of an alkyne with a sp^2 carbon of an aryl or vinyl halide (or triflate) [9]. The classic Pd-catalyzed Sonogashira cross reaction involves the reaction of a halide and a terminal alkyne in the presence of Pd(II) salts such as chloride or acetate and ligands such as phosphines and phosphates, copper salt (as co-catalyst) and an amine to form an aryl acetylene under anaerobic conditions [10, 11]. The products obtained from this reaction can be used for the synthesis of substituted alkynes [7] in the total synthesis of several natural products [12], pharmaceutical complex molecules [13], polymeric and optical materials [14].

Bearing in mind, the high price of palladium salts and ever-growing concerns to protect the environment that demand green chemistry be considered for designing and conducting organic transformations for the synthesis of target molecules. A facile, efficient and eco-friendly strategy for the preparation of the stable palladium species has attracted much attention. In particular low loading Pd-catalyzed Sonogashira cross-coupling reaction has been catalyzed under copper and amine-free reaction condition at atmospheric pressure [15–17].

In spite of superiority and merits of Pd-catalyzed, reactions, the palladium-catalyzed C–C bond formation, suffers from some drawbacks. To circumvent some of these problems, Pd species has been immobilized to various solid supports in order to prepare heterogeneous catalysts with advantages such as easy separation leading to its possible reusability, making it being cost-effective as well as conducted under green conditions [18].

In addition, use of Pd-nano particles (Pd NPs), immobilized onto suitable supports such as silica, polymers or carbon is even more favorable. Such immobilization makes these expensive catalysts recoverable and reusable [1, 19, 20]. Because of good catalytic activity, Pd NP is of great interest with potential to be used as heterogeneous catalysts with unparalleled properties [21, 22]. However, dispersion of the chosen catalytic material on suitable support is still investigated [23].

In a nanocatalyst, surface to volume ratio implies a large number of active sites which participate in reactions [24]. Such nanoparticle-based catalysts are generally attached to solid materials such as graphene [25, 26], graphene oxide (GO) [27, 28], carbon nanotubes [29], activated carbon [30], zeolites [31], silica, or polymeric materials [32] for easy separation. Among these, GO is a promising supporting material for Pd catalysts. GO is a resistant two-dimensional molecule, with the thickness of a carbon atom, but with high strength due to the δ-type bonds and the resonance characteristics in the π-type bonds of the carbons with sp^2 hybridization [33]. GO also has high stability and properties of a low annular tension aromatic polycycle [34]. Furthermore, structural defects in GO can be useful as they make it possible to achieve new surface functionalities which enhance the interactions with the anchored metal nanoparticles [35].

GO is usually synthesized by exfoliation of graphite oxide obtained by oxidation of natural graphite powder with various oxidants in acidic media [36]. Introducing oxygenated groups destroyed the conjugated structure of graphite. Therefore, a heavily oxidized GO is a nonconductor. The oxygen functionalities have been identified as mostly in the form of hydroxyl and epoxy groups on the basal plane and smaller amounts of carboxyl, carbonyl, phenol, lactone, and quinone at the sheet edges, which renders it a good candidate for immobilization of a large number of substances including metals such as Pd, Cu, Pt, *etc.* [37]. The association of NPs immobilized on GO can be prevented and the catalytic activity of NPs-GO can be modified owing to the synergistic interaction between both components. Magnetic nanoparticles supported on various materials have provided new ways to develop recyclable catalyst [38]. Fe_3O_4 nanoparticles are easily synthesized and functionalized by metal and organocatalysts and can be easily separated from the reaction mixture by external magnetic field and reused [39].

In continuation of our study of the preparation of nano metal particles [40–42] and their immobilization on supports especially, GO and magnetic Fe_3O_4 [43–47] as well as our interest in the Sonogashira cross-coupling reaction [48, 49], we introduce a simple, fast and effective strategy for preparation and characterization of palladium(II) immobilized on GO/Fe_3O_4 NPs coated with decorated polyacrylamide and dicyandiamide (Pd@GO/Fe_3O_4/PAA/DCA) as a new magnetic heterogeneous catalyst and its application in Sonogashira C–C cross-coupling reaction as an efficient, green and reusable catalyst.

2. Experimental

2.1. Materials and measurements

The chemicals used for preparation of Pd@GO/Fe_3O_4/PAA/DCA and studying its catalytic activity included graphite powder, iron(III) chloride hexahydrate $FeCl_3{\cdot}6H_2O$, iron(II) chloride tetrahydrate $FeCl_2{\cdot}4H_2O$, 3-(trimethoxysilyl)propyl methacrylate (MAPTMS), acrylamide, potassium peroxydisulfate (KPS), Dicyandiamide (DCA), triethylamine, toluene, $Pd(OAc)_2$, Stevia,halobenzenes, phenylacetylene, propargyl alcohol, K_2CO_3, Cs_2CO_3, KOH, NaOH, distilled water, and EtOH, all provided from Sigma-Aldrich and used as received. All other chemicals and reagents used in the study were analytical grade. The progress of C–C coupling reactions was monitored by using thin layer chromatography (TLC) on commercial aluminum-backed plates of silica gel 60 F254, visualized using ultraviolet light.

The formation of Pd@GO/Fe_3O_4/PAA/DCA was confirmed by characterization techniques, including Fourier transform infrared (FT-IR, Perkin Elmer Spectrum 65 instrument) spectroscopy, X-ray diffraction (XRD, Siemens D5000 with Cu Kα radiation from a sealed tube), scanning electron microscopy (SEM), transmission electron microscopy (TEM), thermogravimetric analysis (TGA, Mettler Toledo instrument with a heating rate of 10 °C min^{-1}, under nitrogen) and vibrating sample magnetometer (VSM, −10,000 to +10,000 Oe at room temperature). The amount of Pd species supported on GO/Fe_3O_4/PAA/DCA was also measured by applying an ICP analyzer (Varian, Vista-pro).

2.2. Synthesis of GO and GO/Fe_3O_4 composite

GO was synthesized from graphite powder as described previously [50]. To synthesize the GO/Fe_3O_4 composite, 0.5 g of synthesized GO was poured in 200 mL of distilled water under stirring for 30 min. After that, 3.5 g of $FeCl_3 \cdot 6H_2O$ was added into the mixture under vigorous stirring and purging of N_2 gas for 30 min. Then, 0.65 g of $FeCl_2 \cdot 4H_2O$ was added into the mixture under N_2 atmosphere. Finally, to this mixture an ammonia solution (25%, 120 mL) was added, diluted by addition of 200 mL water and the suspension was refluxed for 2 h. The GO/Fe_3O_4 composite was dried at 50 °C under vacuum overnight.

2.3. Functionalization of GO/Fe_3O_4 with 3-(trimethoxysilyl)propyl methacrylate (MAPTMS): Synthesis of GO/Fe_3O_4/MAPTMS

To prepare the catalyst, GO/Fe_3O_4 was first functionalized with 3-(trimethoxysilyl)-propyl methacrylate; 1 g of GO/Fe_3O_4 and 1 mL (5 mmol) of MAPTMS were stirred in 25 mL dry toluene under N_2 gas at ambient temperature overnight. After that, the resulting product was magnetically collected and washed several times with toluene and dried at 35 °C overnight in an oven.

2.4. Polymerization and synthesis of GO/Fe_3O_4/PAA nanocomposite

GO/Fe_3O_4/MAPTMS (1.2 g) was suspended in distilled water and sonicated under ultrasonic irradiation (100 W) for 30 min. Subsequently, acrylamide (1.2 g) and KPS (0.6 mg) as the polymerization initiator were added to the reaction mixture and kept at 60 °C for 12 h to complete the polymerization. Finally, the precipitate was filtered and washed with H_2O repeatedly. GO/Fe_3O_4/PAA was achieved after drying for 12 h at 70 °C.

2.5. Conjugation of DCA to GO/Fe_3O_4/PAA: Synthesis of GO/Fe_3O_4/PAA/DCA

GO/Fe_3O_4/PAA/DCA was synthesized by reaction of DCA (0.5 g), triethylamine (0.5 mL), and GO/Fe_3O_4/PAA (1 g) under reflux in H_2O (25 mL) for 24 h. After completion of the reaction, the precipitate was filtered, washed with distilled water several times and dried in an oven for 24 h at 70 °C.

2.6. Immobilization of Pd nanoparticles on GO/Fe_3O_4/PAA/DCA by using Stevia as a reducing agent: Pd@GO/Fe_3O_4/PAA/DCA

To incorporate Pd nanoparticles on GO/Fe_3O_4/PAA/DCA, GO/Fe_3O_4/PAA/DCA (1.2 g) was suspended in distilled water (15 mL) containing $Pd(OAc)_2$ (0.02 g) and then stirred at ambient temperature for 12 h. Then, a solution of Stevia in methanol (10 mL) was added to the reaction mixture and stirred for five more hours. The final product (Pd@GO/Fe_3O_4/PAA/DCA) was obtained by an external magnet, washing (three times with methanol) and drying in the oven at 60 °C overnight (Scheme 1).

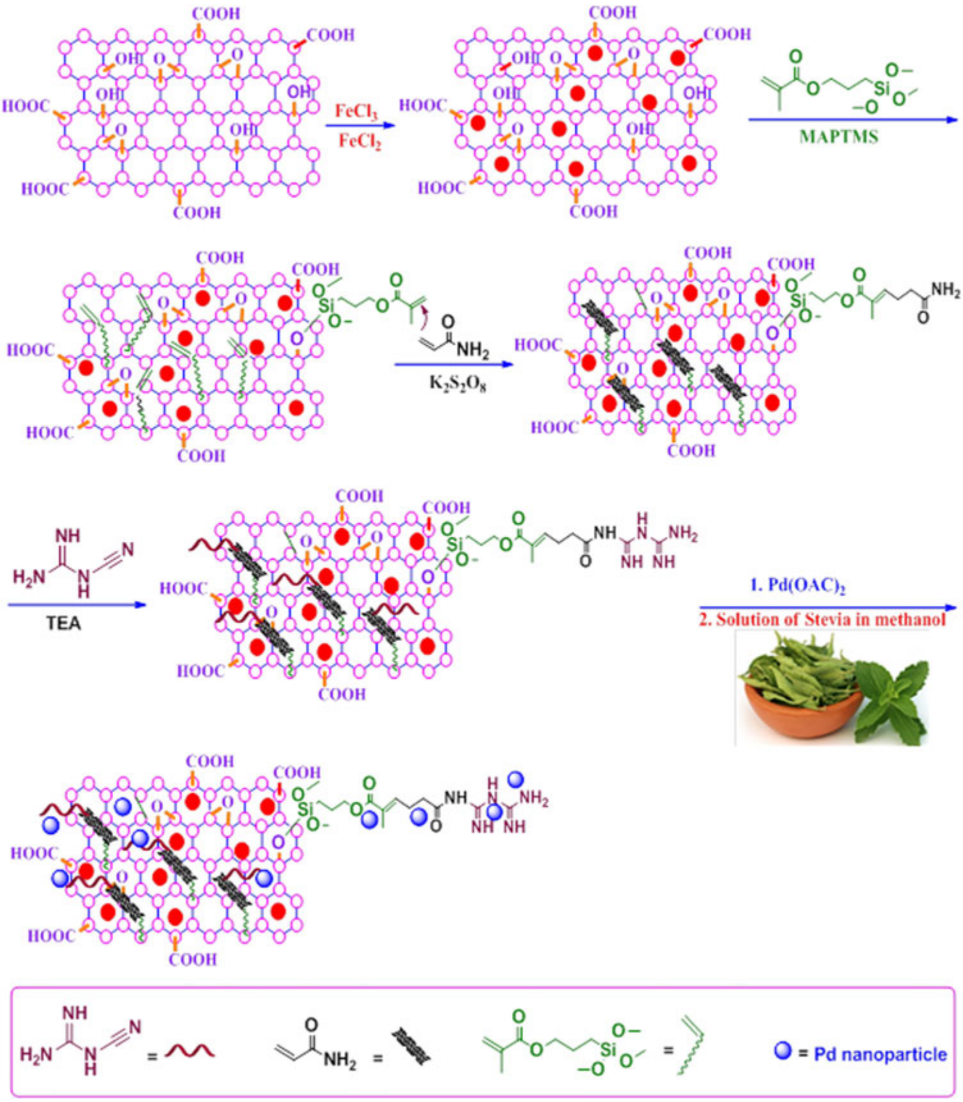

Scheme 1. The schematic route for preparation of Pd@GO/Fe_3O_4/PAA/DCA.

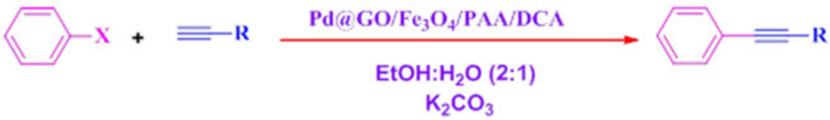

Scheme 2. Sonogashira reaction in the presence of Pd@GO/Fe_3O_4/PAA/DCA.

2.7. Typical procedure for Sonogashira reaction

Pd@GO/Fe_3O_4/PAA/DCA (10 mol%) and K_2CO_3 (3 mmol) were added to a mixture of halobenzene (1 mmol) and acetylene (1.2 mmol) in water:EtOH (2:1) as the solvent (Scheme 2). The reaction mixture was then refluxed for appropriate reaction time. The progress of the reaction was monitored by TLC. At the end of the reaction, the catalyst was filtered by an external magnet. After that, the organic layer was extracted with diethyl ether and purified by column chromatography over silica gel by using hexane/ethyl acetate (4:1) as eluent to furnish the corresponding product. Upon completion of the coupling reaction, to recycle the catalyst, the recovered catalyst was washed with EtOH two times and dried in the oven at 90 °C overnight.

3. Results and discussion

The goal of this study was developing a new GO support decorated with acrylamide, dicyandiamide, and Fe_3O_4 for immobilization of Pd(0). Using Fe_3O_4 leads to easy separation of the catalyst from the reaction medium with an external magnet after completion of the reaction. At first, GO was prepared from graphene using Hummer's method [50]. Then, graphene magnesium oxide was obtained by using $FeCl_2{\cdot}4H_2O$ and $FeCl_3{\cdot}6H_2O$ salts. The surface of magnetic GO was modified using MAPTMS, leading to formation of C[dbond]C bonds on GO. Subsequently, acrylamide and dicyandiamide were used to produce the polymeric network. Pd(II) salt was then added to GO/Fe_3O_4/PAA/DCA, reduced by Stevia and finally Pd@GO/Fe_3O_4/PAA/DCA was obtained.

3.1. Catalyst characterization

FTIR spectroscopy was employed to establish the structure of Pd@GO/Fe_3O_4/PAA/DCA (Figure 1). FTIR spectra of GO/Fe_3O_4, GO/Fe_3O_4/MAPTMS, GO/Fe_3O_4/PAA and GO/Fe_3O_4/PAA/DCA were also recorded and compared with that of GO/Fe_3O_4/PAA/DCA. In the FTIR spectrum of GO/Fe_3O_4, the bands at 3393, 1617, 1047, and 587 cm^{-1} indicate –OH group vibration, C = O stretching vibration of carbonyl, C – O stretching group of alkoxy and Fe–O stretching vibration, respectively.

In GO/Fe_3O_4/MAPTMS (Figure 1(b)), bands as a broad peak between 1050 and 1116 cm^{-1} indicate vibration of Si–O–Si. The presence of the vibration bands at 2924, 1715, 1633, and 1166 cm^{-1} which can be assigned, respectively, to CH_2, C[dbond]O, C[dbond]C, and C✇O stretching can prove functionalization of MAPTM to the surface of GO/Fe_3O_4. After the polymerization step, bands at 1634 cm^{-1} and 3250–3450 cm^{-1} are due to $CONH_2$ and NH, respectively (Figure 1).

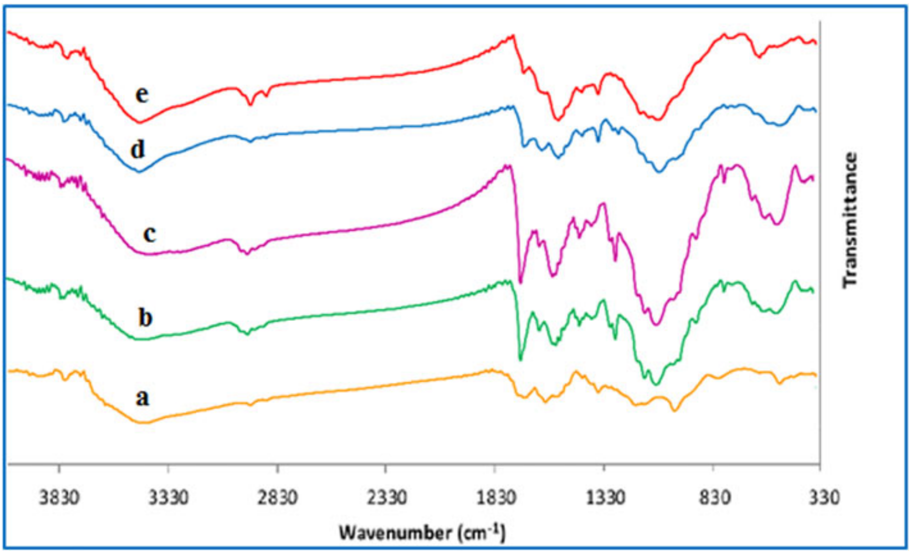

Figure 1. The FTIR spectra of (a) GO/Fe_3O_4, (b) GO/Fe_3O_4/MAPTMS, (c) GO/Fe_3O_4/PAA, (d) GO/Fe_3O_4/PAA/DCA, and (e) Pd@GO/Fe_3O_4/PAA/DCA.

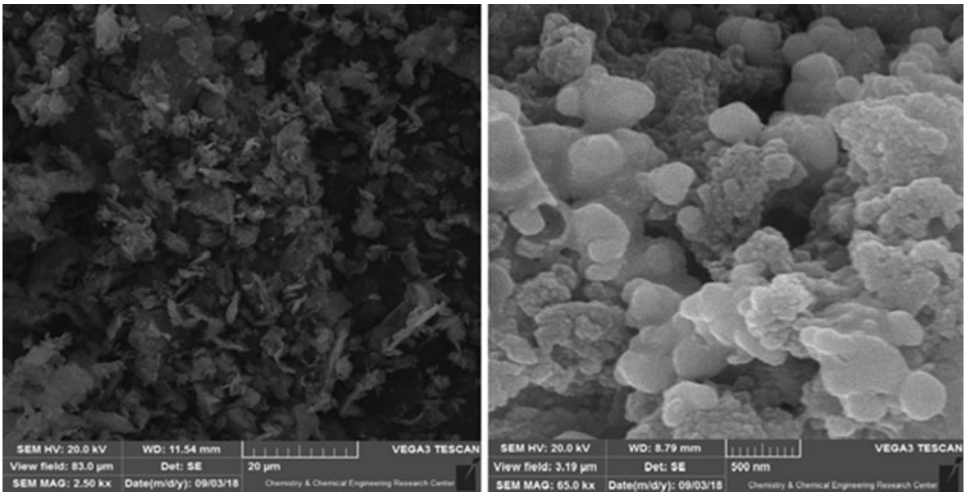

Figure 2. SEM images of (a) GO and (b) Pd@GO/Fe_3O_4/PAA/DCA.

The FT-IR spectrum of GO/Fe_3O_4/PAA/DCA (Figure 1) also possesses the characteristic bands of GO/Fe_3O_4, implying that the structure of GO/Fe_3O_4 is preserved upon chemical functionalization with PAA and DCA. Moreover, additionally, the non-observation of the CN peak in 2230 represents connection of DCA to GO/Fe_3O_4/PAA.

The morphology of Pd@GO/Fe_3O_4/PAA/DCA was studied by recording the SEM images of the catalyst (Figure 2). As depicted, upon decoration of polyacrylamide and incorporation of DCA and Pd nanoparticles, the morphology of GO is preserved. Compared to GO, Pd@GO/Fe_3O_4/PAA/DCA showed more compact morphology, which can stem from intertwining of the polymeric chain.

TEM image of Pd@GO/Fe_3O_4/PAA/DCA (Figure 3) shows that Fe_3O_4 and Pd nanoparticles were distributed between the GO layers.

The Pd@GO/Fe_3O_4/PAA/DCA catalyst was also studied using EDX analysis (Figure 4). As can be seen, EDX analysis illustrates presence of all the elements (O, C, N, Fe, Si and Pd) onto the GO sheets.

XRD analysis, as a method for studying the structure of the catalyst, was also employed to characterize the Pd@GO/Fe_3O_4/PAA/DCA (Figure 5). XRD patterns of GO/Fe_3O_4 and Pd@GO/Fe_3O_4/PAA/DCA were obtained. Peaks at $2\theta = 30.10°$ (220), 35.10° (311), 43.4° (400), 51.70° (422), 57.40° (511), and 62.61° (440) can be attributed to the structure of Fe_3O_4. Comparing the XRD patterns of the catalyst and GO/Fe_3O_4 reveals some additional peaks at $2\theta = 40.10$ (110), 46.521 (200), and 68.25 (220), confirming the presence of palladium.

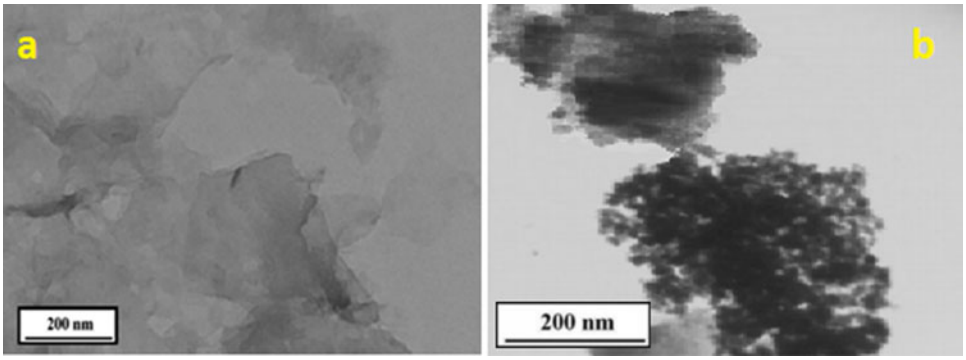

Figure 3. TEM images of Pd@GO/Fe_3O_4/PAA/DCA.

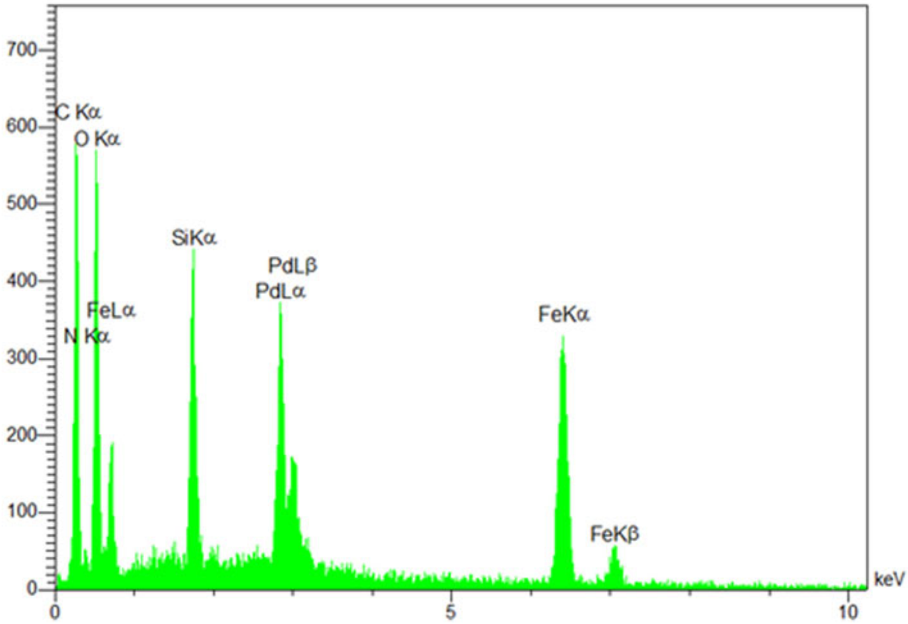

Figure 4. EDX analysis of Pd@GO/Fe_3O_4/PAA/DCA.

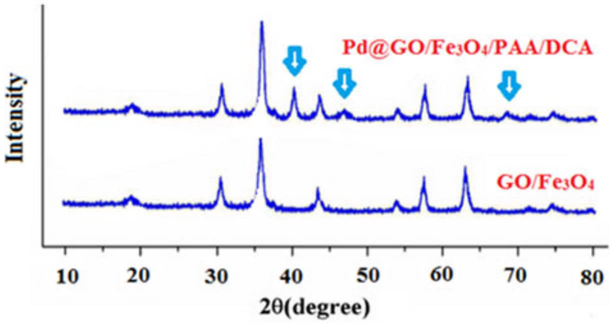

Figure 5. The XRD patterns of Pd@GO/Fe_3O_4/PAA/DCA.

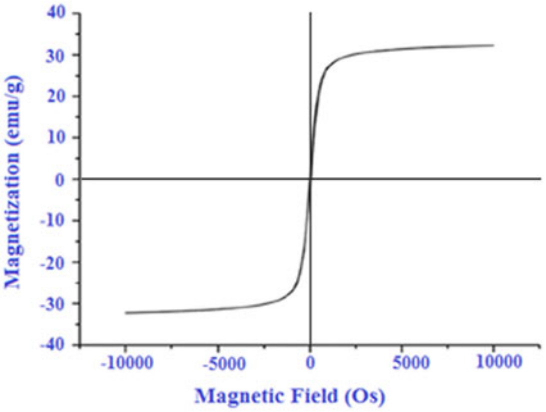

Figure 6. Room-temperature magnetization *curve* of Pd@GO/Fe_3O_4/PAA/DCA.

The magnetic properties of the Pd@GO/Fe_3O_4/PAA/DCA catalyst were determined with a vibrating sample magnetometer (VSM) from −10,000 to +10,000 Oe at room temperature. The magnetization hysteresis loop of the composite was an S-like curve, indicating that the composite was superparamagnetic (Figure 6). The saturation magnetization character of Pd@GO/Fe_3O_4/PAA/DCA was sufficient to ensure the easy and quick separation of the compound from solutions.

The content of Pd nanoparticles in Pd@GO/Fe_3O_4/PAA/DCA was measured by using ICP-AES analysis. To prepare the sample for analysis, Pd@GO/Fe_3O_4/PAA/DCA was fully digested in concentrated hydrochloric and nitric acids mixture. Then, the extract was subjected to the ICP-AES analysis. Using this method, the content of Pd in Pd@GO/Fe_3O_4/PAA/DCA was calculated to be 2.47 w/w%.

Thermal stability of Pd@GO/Fe_3O_4/PAA/DCA was also investigated by using TGA analysis (Figure 7). The thermogram of Pd@GO/Fe_3O_4/PAA/DCA exhibited several weight losses. Thermogravimetric analysis (TGA) of GO/Fe_3O_4 (a) and Pd@GO/Fe_3O_4/PAA/DCA nanocomposite (b) was further used to study the composition of the nanocomposite. The TGA of both materials show three main weight losses. In the thermogram of GO/Fe_3O_4, these three steps observed at 100 °C, 160–240 °C, and 380–440 °C are attributed to the loss of water, dehydration of surface oxygen and hydroxyl groups in GO decomposition of graphene structure, respectively.

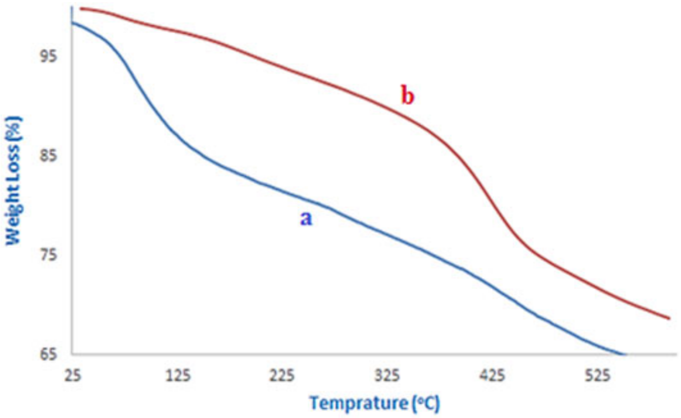

Figure 7. The TGA analysis of (a) GO/Fe_3O_4 and (b) Pd@GO/Fe_3O_4/PAA/DCA.

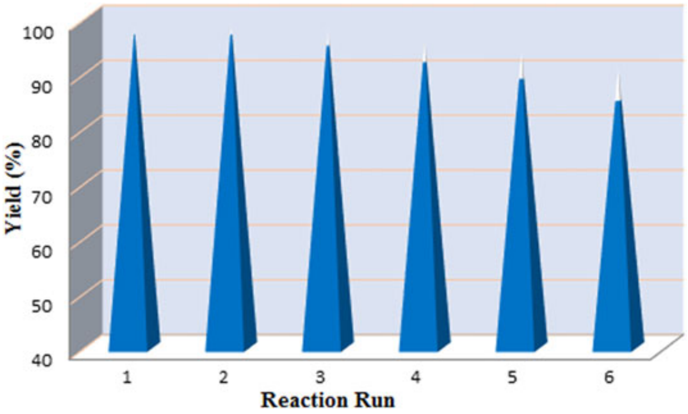

Figure 8. Reusability of the Pd@GO/Fe_3O_4/PAA/DCA.

In the thermogram of Pd/GO/Fe_3O_4/PAA/DCA, the first weight loss at 100 °C was attributed to desorption of water. The second weight loss from 200 °C to 300 °C is due to dehydration of surface oxygen and hydroxyl groups in GO. The final weight loss around 400–450 °C indicates decomposition of the graphene structure. (Figure 7 The comparison of the thermograms exhibits that the content of organosilane and polymer were about 5.6 and 23.57 w/w%, respectively.

3.2. Catalytic activity

Catalytic activity of Pd@GO/Fe_3O_4/PAA/DCA was investigated for Sonogashira C–C coupling for synthesis of alkyne derivatives from the reaction of halobenzene and acetylene in the absence of copper co-catalyst and ligand. The reaction of phenylacetylene and iodobenzene was selected as a model reaction and used for optimization of the reaction variables such as solvent, temperature, base and catalyst amount (Table 1). Comparing the yields of the model product in the presence of various

Table 1. Optimization of reaction conditions for Sonogashira coupling reaction of iodobenzene with phenylacetylene.

Entry	Reaction condition[a]	Time (h)	Catalyst amount (mol %)	Base	Yield (%)[b]
1	H_2O/ r.t	2.2	10	K_2CO_3	71
2	EtOH/ r.t	2.5	10	K_2CO_3	68
3	H_2O/ 50 °C	2	10	K_2CO_3	80
4	EtOH/ 50 °C	2	10	K_2CO_3	82
5	H_2O/ 96 °C	2	10	K_2CO_3	94
6	EtOH/ 87 °C	2	10	K_2CO_3	90
7	CH_3OH/ 60 °C	2.5	10	K_2CO_3	83
8	CH_3CN/ 83 °C	2.2	10	K_2CO_3	87
9	$CHCl_3$/ 61 °C	2.5	10	K_2CO_3	80
10	Toluene	2.5	10	K_2CO_3	81
11	H_2O–EtOH (1:1)/ 72	2	10	K_2CO_3	90
12	H_2O–EtOH (2:1)/ 86	1.8	10	K_2CO_3	97
13	H_2O–EtOH (2:1)/ 86	1.8	15	K_2CO_3	95
14	H_2O–EtOH (2:1)/ 86	2.2	5	K_2CO_3	82
15	H_2O–EtOH (2:1)/ 86	1.8	10	KOH	80
16	H_2O–EtOH (2:1)/ 86	2.5	10	NaOH	82

[a] Reaction were run in 5 mL of solvent with 1 mmol of iodobenzene, 1.2 mmol of phenylacetylene, and 3 mmol of base.

[b] Isolated yield.

solvents such as acetonitrile, toluene, water, chloroform, and H_2O/EtOH showed that the mixture of water and ethanol is the best choice for this reaction.

Eventually, use of K_2CO_3 as the base, H_2O:EtOH (2:1) as the solvent, and 10 mol% of the catalyst at 86 °C led to high yield of the model product.

We report a highly selective method for preparation of various derivatives of diarylethynes by using of Pd@GO/Fe_3O_4/PAA/DCA in a modified Sonogashira reaction. In contrast to the original Sonogashira method, very little Glaser Coupling product was formed. Also, this method reduces the need to use excess arylethyne to promote the cross-coupling efficiency.

In the following, the effect of the number of surface nitrogens on the catalytic activity of the final catalyst was investigated. To this purpose, another catalyst, Pd@GO/Fe_3O_4/PAA, was prepared and its catalytic efficiency in the synthesis of the model product was checked.

The results showed that the order of the yield of the desired product in the presence of various catalysts varied in the following order: Pd@GO/Fe_3O_4/PAA/DCA (97%) $>$ Pd@GO/Fe_3O_4/PAA (60%) (Table 2). The difference of catalytic activity can be attributed to the different loading of Pd nanoparticle on the catalyst. To verify this assumption and estimate the loading of Pd, two prepared catalysts were subjected to ICP analysis. Loading of Pd in Pd@GO/Fe_3O_4/PAA/DCA was the highest (2.47 w/w%) while Pd@GO/Fe_3O_4/PAA showed lower Pd content (0.10 w/w%), showing the role of the number of surface nitrogens in anchoring Pd nanoparticles. Having the optimized reaction conditions, the generality of this methodology was confirmed by applying different alkynes and aryl halides with electron-withdrawing and electron-donating groups.

Finally, catalytic activity of this system was used in Sonogashira cross coupling and the result compared with those of some previously reported catalysts (Table 3). The new palladium complex as a magnetic catalyst takes advantage of both magnetic and functionalized surface. Recoverability, reusability, and easy separation of magnetic

Table 2. $Pd@GO/Fe_3O_4/PAA/DCA$ catalyzed Sonogashira reaction of various halides with terminal alkynes.[a]

Entry	Aryl halide	Terminal alkyne	Product	Time (h)	Yield[b] (%)
1	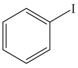	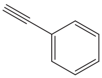	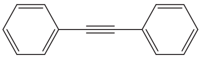	1.8	97
2	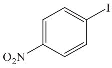	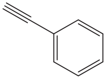	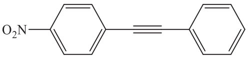	2	95
3	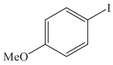	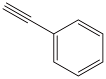	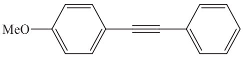	2.2	91
4	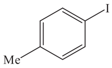	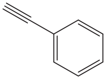	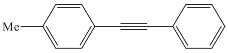	1.8	94
5	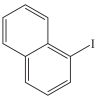	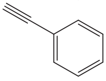	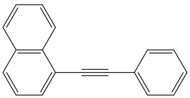	3.5	85
6	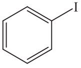	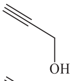	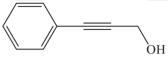	2.8	91
7	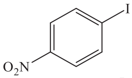	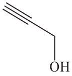	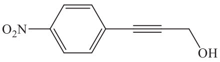	1.8	94
8	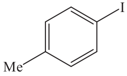	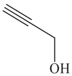	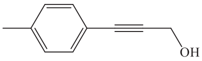	3.2	87
9	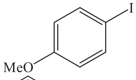	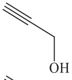	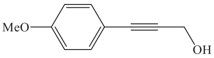	2.8	89
10	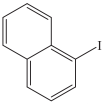	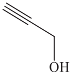	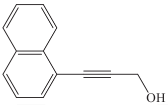	3.5	85
11	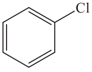	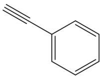	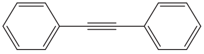	4	82
12	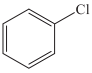	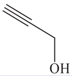	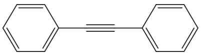	4.5	80

[a]Reaction condition: aryl halide (1.0 mmol), terminal alkyne (1.2 mmol), $Pd/GO/Fe_3O_4/PAA/DCA$ (10 mol%) and K_2CO_3 (3.0 mmol) in H_2O:EtOH (2:1) at 86 °C.
[b]Isolated yield.

nanocatalyst, and performing the reaction in a benign solvent are among the remarkable advantages of the proposed synthetic method.

Comparison of the catalytic activity of $Pd@GO/Fe_3O_4/PAA/DCA$ with other catalysts showed the comparative catalytic activity of our catalyst. This catalyst also could promote the model reaction in the presence of cost-effective and nontoxic K_2CO_3 as base in EtOH:H_2O as green solvent while some of the tabulated catalysts required expensive (Table 3, entry 1) or toxic bases (Table 3, entry 11) and/or solvents (Table 3, entries 2, 3, 5, 7, and 9–11). Furthermore, the reaction time and temperature required for completion of this reaction in the presence of $Pd@GO/Fe_3O_4/PAA/DCA$ catalysis were lower or comparative to the catalysts tabulated in Table 3 (entries 2, 3, 4, 5, and 7–12).

The properties which make our research better than previous procedures are mild reaction conditions, environmentally benign, simple recycle of the nanocatalyst by an

Table 3. Comparison of Pd@GO/Fe_3O_4/PAA/DCA with heterogeneous catalysts.

Entry	Catalyst	Time (h)	Temp. (°C)	Yield (%)	Solvent	Base	Ref.
1	$[Pd(dppe)(OTf)_2]$	24	60	70	CH_3OH	Cs_2CO_3	[51]
2	$[(P{\wedge}C)PdCl_2]^a$	6	130	81	DMF	K_2CO_3	[52]
3	$[(C{\wedge}C)PdCl_2]^b$	4.5	130	87	DMF	K_2CO_3	[52]
4	$NiCl_2.6H_2O$	2	120	86	EG	NaOH	[53
5	$FeCl_3.PPh_3$	48	135	99	Toluene	K_3PO_4	[54]
6	$PdCl_2\{C(N(H)\text{-}NPh_2)@N(H)Cy\}(C,,NCy)$	2	80	95	EtOH	K_2CO_3	[55]
7	$[(Pd\{k^2\text{-}C,N)\text{-}(3\text{-}(dimethylaminomethyl)indole)\}\mu\text{-}OAc)_2]$	3	120	85	DMF/H_2O	K_2CO_3	[56]
8	Et_2Zn/DMEDA	48	125	54	Dioxane	K_3PO_4	[57]
9	CuI/L^c	6	145	90	DMF	K_2CO_3	[58]
10	$[N\text{-}benzyl\ DABCO]^+[Cu_4Cl_5]^-$	3	135	55	DMF	K_2CO_3	[59]
11	$Cu(OAc)_2$	24	140	65	Et_3N	Et_3N	[60]
12	Pd@Hal-2N-TCT-EDA	2	90	95	EtOH	K_2CO_3	[61]
13	$[PdCl_2(NH_2CH_2COOH)_2$	2	60	93	H_2O:acetone	NaOH	[62]
13	Pd@GO/Fe_3O_4/PAA/DCA	1.8	80	97	EtOH:H_2O	K_2CO_3	This work

Reaction of iodobenzene with phenylacetylene.

[a] Five-membered palladacycle.

[b] Seven-membered analogs.

[c] N,N`-dibenzyl BINAM.

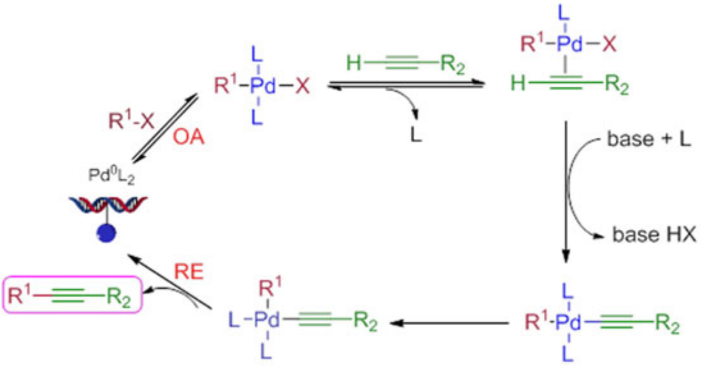

Scheme 3. Plausible reaction mechanism.

external magnet and reusability of the catalyst without considerable loss of catalytic activity.

3.3. Reusability of the catalyst

Considering the importance of simple recovery and recyclability of heterogeneous catalysts, the recyclability of Pd@GO/Fe_3O_4/PAA/DCA for catalyzing the model reaction was investigated. After completion of each cycle, the catalyst was separated easily by an external magnet. The catalyst was recovered, washed with EtOH, and recycled for six reaction runs and the yields of the model product in the presence of the fresh and recycled Pd@GO/Fe_3O_4/PAA/DCA were compared. Results showed no significant loss in activity of catalyst after six reaction runs (about 0.008).

A plausible reaction mechanism is proposed in Scheme 3. In accordance with this suggested mechanistic pathway, initially [Pd(0)L_2] is oxidatively added to the aryl or vinyl halide. Then, a reversible coordination of the alkyne occurs, generating an alkyne–Pd(II) complex where the acetylenic proton is removed by the base along with coordination of the acetylene ligand to the metal. This [Pd(II)R^1(C[tbond]CR^2)L_2] complex releases the cross-coupled product by reductive elimination regenerating the catalyst species [Pd(0)L_2].

4. Conclusion

A hybrid catalyst, Pd@GO/Fe_3O_4/PAA/DCA, has been prepared by reacting functionalized GO/Fe_3O_4 with acrylamide and dicyandiamide, followed by immobilization of Pd(0) nanoparticles. Pd@GO/Fe_3O_4/PAA/DCA catalyzed Sonogashira coupling in the absence of copper and ligand under mild reaction conditions. To study the effect of nitrogen atoms on the surface of GO, Pd@GO/Fe_3O_4/PAA was synthesized and compared with Pd@GO/Fe_3O_4/PAA/DCA. The results show that Pd@GO/Fe_3O_4/PAA/DCA has better performance due to the higher number of nitrogen atoms on GO.

Acknowledgments

The authors gratefully recognize partial financial support from Alzahra, University research council.

Disclosure statement

No potential conflict of interest was reported by the authors.

References

[1] N.Y. Baran. *J. Mol. Struct.*, **1176**, 266 (2019).
[2] B.H. Lipshutz, T. Butler, E. Swift. *Org. Lett.*, **10**, 697 (2008).
[3] F.-S. Han. *Chem. Soc. Rev.*, **42**, 5270 (2013).
[4] A.O. King, N. Okukado, E.-i. Negishi. *J. Chem. Soc. Chem. Commun.*, 683 (1977).
[5] I.P. Beletskaya, A.V. Cheprakov. *Chem. Rev.*, **100**, 3009 (2000).
[6] T.J. Colacot. *Platin. Met. Rev.*, **55**, 84 (2011).
[7] L. Cassar. *J. Organomet. Chem.*, **93**, 253 (1975).
[8] H. Dieck, F. Heck. *J. Organomet. Chem.*, **93**, 259 (1975).
[9] K. Sonogashira, Y. Tohda, N. Hagihara. *Tetrahedron Lett.*, **16**, 4467 (1975).
[10] R. Chinchilla, C. Nájera. *Chem. Soc. Rev.*, **40**, 5084 (2011).
[11] M.M. Heravi, S. Sadjadi. *Tetrahedron*, **37**, 7761 (2009).
[12] K. Nicolaou, W.M. Dai. *Angew. Chem. Int. Ed. Engl.*, **30**, 1387 (1991).
[13] N.D. Cosford, L. Tehrani, J. Roppe, E. Schweiger, N.D. Smith, J. Anderson, L. Bristow, J. Brodkin, X. Jiang, I. McDonald. *J. Med. Chem.*, **46**, 204 (2003).
[14] V. Francke, T. Mangel, K. Müllen. *Macromolecules*, **31**, 2447 (1998).
[15] M. Esmaeilpour, A.R. Sardarian, H. Firouzabadi. *J. Organomet. Chem.*, **873**, 22 (2018).
[16] M. Khajehzadeh, M. Moghadam, S. Jamehbozorgi. *Inorg. Chim. Acta*, **485**, 173 (2019).
[17] F. Zhu, P. Zhao, Q. Li, D. Yang. *J. Organomet. Chem.*, **859**, 92 (2018).
[18] X. Liu, D. Astruc. *Adv. Synth. Catal.*, **360**, 3426 (2018).
[19] S. Sadjadi, M. Malmir, M.M. Heravi, F.G. Kahangi. *Int. J. Biol. Macromol.*, **118**, 1903 (2018).
[20] M. Renuka, V. Gayathri. *J. Organomet. Chem.*, **874**, 26 (2018).
[21] Q. Wang, X. Jing, J. Han, L. Yu, Q. Xu. *Mater. Lett.*, **215**, 65 (2018).
[22] E. Ghonchepour, M.R. Islami, A.M. Tikdari. *J. Organomet. Chem.*, **883**, 1 (2019).
[23] R.Y. Parapat, O.H. Saputra, A.P. Ang, M. Schwarze, R. Schomäcker. *RSC Adv.*, **4**, 50955 (2014).

[24] G. Zhan. *Chem. Eng. J.*, **355**, 320 (2019).
[25] Y. Yang, A.C. Reber, S.E. Gilliland, C.E. Castano, B.F. Gupton, S.N. Khanna. *J. Catal.*, **360**, 20 (2018).
[26] T. Revathy, S. Dhanavel, T. Sivaranjani, V. Narayanan, T. Maiyalagan, A. Stephen. *Appl. Surf. Sci.*, **449**, 764 (2018).
[27] J.C. Ng, C.Y. Tan, B.H. Ong, A. Matsuda, W.J. Basirun, W.K. Tan, R. Singh, B.K. Yap. *Mater. Res. Bull.*, **112**, 213 (2019).
[28] N. Shang, C. Feng, H. Zhang, S. Gao, R. Tang, C. Wang, Z. Wang. *Catal. Commun.*, **40**, 111 (2013).
[29] M. Feng, Z.-H. Luo, R.-Q. Chen, S. Yi, H. Lu, G.-P. Cao, C. Lu, S.-Y. Feng, C.-Y. Li. *Appl. Catal. A*, **570**, 329 (2019).
[30] J. Zhou, Z. Lou, J. Xu, X. Zhou, K. Yang, X. Gao, Y. Zhang, X. Xu. *Chem. Eng. J.*, **358**, 1176 (2019).
[31] X. Jia, D. Jiang, D.C. Tsang, J. Choi, A.C. Yip. *Microporous Mesoporous Mater.*, **276**, 147 (2019).
[32] Z.-W. Ye, W.-B. Yi. *J. Fluorine Chem.*, **129**, 1124 (2008).
[33] K. Kelly, W. Billups. *Acc. Chem. Res.*, **46**, 4 (2012).
[34] D.C. Marcano, D.V. Kosynkin, J.M. Berlin, A. Sinitskii, Z. Sun, A. Slesarev, L.B. Alemany, W. Lu, J.M. Tour. *ACS Nano.*, **4**, 4806 (2010).
[35] S. Kumar, S. Chinnathambi, N. Munichandraiah. *New J. Chem.*, **39**, 7066 (2015).
[36] A. Moreno-Bárcenas, J.F. Perez-Robles, Y.V. Vorobiev, I.E. Pech-Pech , A. García. *Int. J. Electrochem. Sci.*, **13**, 3171 (2018).
[37] C. Huang, C. Li, G. Shi. *Energy Environ. Sci.*, **5**, 8848 (2012).
[38] S. Guo, G. Zhang, Y. Guo, J.C. Yu. *Carbon*, **60**, 437 (2013).
[39] S. Schweizer, J.-M. Becht, C. Le Drian. *Tetrahedron*, **66**, 765 (2010).
[40] R. Sedghi, S. Asadi, B. Heidari, M.M. Heravi. *Mater. Res. Bull.*, **92**, 65 (2017).
[41] S. Sadjadi, M.M. Heravi, M. Malmir, F. Noritajer. *Mater. Chem. Phys.*, **223**, 380 (2019).
[42] S. Sadjadi, S. Samadi, M. Samadi. *Res. Chem. Intermed.*, **45**, 2441 (2019).
[43] S. Asadi, R. Sedghi, M.M. Heravi. *Catal. Lett.*, **147**, 2045 (2017).
[44] B. Heidari, M.M. Heravi, M.R. Nabid, R. Sedghi, S.E. Hooshmand. *Appl. Organomet. Chem.*, **33**, e4632 (2019).
[45] S. Sadjadi, M.M. Heravi, M. Raja. *Int. J. Biol. Macromol.*, **122**, 228 (2019).
[46] S. Sadjadi, M. Malmir, M.M. Heravi. *Appl. Clay Sci.*, **168**, 184 (2019).
[47] S. Sadjadi, M. Malmir, M.M. Heravi, F.G. Kahangi. *Inorg. Chim. Acta*, **488**, 62 (2019).
[48] S. Sadjadi, M. Malmir, M.M. Heravi, M. Raja. *Int. J. Biol. Macromol* , **128**, 638 (2019).
[49] S. Sadjadi, M. Akbari, B. Léger, E. Monflier, M.M. Heravi. *ACS Sustain. Chem. Eng.*,**7**, 6720 (2019).
[50] W.S. Hummers Jr., R.E. Offeman. *J. Am. Chem. Soc.*, **80**, 1339 (1958).
[51] A. Komáromi, G.L. Tolnai, Z. Novák. *Tetrahedron Lett.*, **49**, 7294 (2008).
[52] B. Ghanbari, L. Shahhoseini, H. Hosseini, M. Bagherzadeh, A. Owczarzak, M. Kubicki. *J. Organomet. Chem.*, **866**, 72 (2018).
[53] M. Bakherad, A. Keivanloo, S. Samangooei. *Chin. J. Catal.*, **35**, 324 (2014).
[54] D.N. Sawant, P.J. Tambade, Y.S. Wagh, B.M. Bhanage. *Tetrahedron Lett.*, **51**, 2758 (2010).
[55] S.J. Sabounchei, M. Ahmadi. *Catal. Commun.*, **37**, 114 (2013).
[56] N. Nowrouzi, M. Zarei. *Tetrahedron*, **71**, 7847 (2015).
[57] K. Thakur, E. Jaseer, A.B. Naidu, G. Sekar. *Tetrahedron Lett.*, **50**, 2865 (2009).
[58] S.J. Sabounchei, M. Ahmadi, Z. Nasri, E. Shams, M. Panahimehr. *Tetrahedron Lett.*, **54**, 4656 (2013).
[59] K. Karami, N.H. Naeini. *Turk. J. Chem.*, **39**, 1199 (2015).
[60] R.N. Prabhu, S. Pal. *Tetrahedron Lett.*, **56**, 5252 (2015).
[61] S. Sadjadi, M.M. Heravi, B. Masoumi, S.S. Kazemi. *J. Coord. Chem.*, **72**, 119 (2019).
[62] M.-P. Guo, S.-W. Liu, S.-B. Chen, Y.-J. Wen, H. Liang, M.-Y. Lv. *Synth. Commun.*, **45**, 767 (2015).